*International Journal of Pharmaceutics*, 86 (1992) 221–230



IJP 02875

# Solid-state properties of drugs. III. Differential scanning calorimetry of chiral drug mixtures existing as racemic solid solutions, racemic mixtures or racemic compounds

M. Elsabee [b] and R.J. Prankerd [a]

[a] *Department of Pharmaceutics, College of Pharmacy, University of Florida, J. Hillis Miller Health Center, Gainesville, FL 32610 (USA) and* [b] *Department of Chemistry, University of Cairo, Cairo (Egypt)*

(Received 21 January 1992)
(Modified version received 27 April 1992)
(Accepted 28 April 1992)

*Key words*: DSC; Deconvolution; Enthalpy of fusion; Solid-liquid phase diagram; Chiral drug; Grinding; Infrared spectroscopy; Minor component detection; Peak asymmetry; Chiral purity

## Summary

A previously reported method for peak shape analysis and deconvolution of overlapping endotherms in differential scanning calorimetry (DSC) data has been applied to binary mixtures of the enantiomers of a chiral drug and of two model compounds. The chiral substances represented the three types of known phase behavior for chiral compounds, i.e., racemic solid solutions (camphorquinone), racemic mixtures (propranolol hydrochloride) and racemic compounds (mandelic acid). Phase diagrams based on enthalpies of fusion ($\Delta H_f^m$) for camphorquinone and propranolol hydrochloride were as easy to interpret as those based on melting behavior. However, the phase diagram based on $\Delta H_f^m$ for mandelic acid was much easier to interpret than the melting behavior phase diagram. Formation of the racemic compound of mandelic acid by thorough grinding of mixtures of the enantiomers was demonstrated by DSC and infrared spectra. A novel, fast method of chiral purity determination is suggested for propranolol hydrochloride. The DSC endotherm peak asymmetry was shown to be a linear function of enantiomeric composition in the range 85–100 mol%. This approach may also be applicable to chiral mixtures of other drugs.

## Introduction

The quantitative interpretation of differential scanning calorimetry (DSC) scans is made difficult or even impossible in many cases by the presence of overlapping endotherms or exotherms from multiple thermal events (e.g., fusion, polymorphic transition, vapor desorption, decomposition) which occur in the same temperature range. An approach to deconvolution of such DSC curves is presented in the preceding paper (Elsabee and Prankerd, 1992), using a commercial multiple non-linear regression analysis program (PeakFit®). This approach allowed construction of a solid-liquid phase diagram from the changes in enthalpy for fusion ($\Delta H_f^m$) of mixtures of (1*S*,2*R*)-(+)- and (1*R*,2*S*)-(−)-ephedrine hydro-

*Correspondence to:* R.J. Prankerd, Department of Pharmacy, University of Queensland, St. Lucia, Brisbane, QLD 4072, Australia.

chloride. It was shown that a chiral mixture containing as little as 1.5% of one isomer of ephedrine hydrochloride could be distinguished from the pure isomer by DSC. The advantages of DSC examination of chiral mixtures include speed, requirements for minimal amounts of material (1–5 mg) and sensitivity. In particular, a DSC study could be performed more quickly than the time needed to set up a chiral HPLC separation, although it is expected that the two methods should be complementary.

The present study examines the application of this approach to mixtures of other chiral drugs (propranolol hydrochloride) or model compounds (camphorquinone and mandelic acid). Such mixtures could arise in manufacturing processes during resolution of racemic synthetic reaction products (by chiral chromatography or by stereospecific recrystallization), from accidental contamination, or by design. The characterization of chiral drugs is presently receiving much increased attention from manufacturing and regulatory organizations, due to the increased recognition of possible differences in absorption and metabolism of optical antipodes, as well as long recognized differences in their pharmacology (Hutt, 1991).

The racemic modifications of chiral substances occur in three types: (1) racemic solid solutions; (2) racemic mixtures; or (3) racemic compounds (Eliel, 1962). Racemic solid solutions display solid-state behavior which is ideal (or nearly so), in contrast to the other two types. Hence, individual crystals contain both the (+)- and (−)- forms of the substance. Racemic mixtures occur when molecules of the (+)- form have greater affinity for each other than for the (−)- form and vice versa. These exist as eutectic mixtures of minute crystals (conglomerates) of the two individual forms. Racemic compounds occur when the (+)- form has a greater affinity for the (−)- form than for other molecules of the (+)- form. This results in the formation of crystals which have a 1:1 ratio of the (+)- and (−)- forms, and which have different physical properties from those of either of the optical antipodes (Eliel, 1962).

Theoretical aspects of the analysis of peak shapes and the deconvolution of overlapping DSC endotherms are presented in the preceding article (Elsabee and Prankerd, 1992). The peak shapes may be either Gaussian or exponentially modified Gaussian (EMG) distributions. Gaussian and EMG distributions obey the following expressions (Eqns 1 and 2), respectively:

$$y = a_0 \exp\left[ -\frac{\left\{ \frac{x - a_1}{a_2} \right\}^2}{2} \right] \tag{1}$$

$$y = f(x) = a_0 \exp\left[ \frac{a_2^2}{2a_3^2} + \frac{a_1 - x}{a_3} \right] \times \left[ \operatorname{erf}\left\{ \frac{x - a_1}{\sqrt{2}\, a_2} - \frac{a_2}{\sqrt{2}\, a_3} \right\} + 1 \right] \tag{2}$$

where $y$ is the measured heat flux for each temperature point on the DSC scan, $x$ denotes the temperature for each heat flux measurement, $a_0$ is the peak amplitude (in Eqn 1 only), $a_1$ represents the peak center, $a_2$ is the peak standard deviation, $a_3$ corresponds to a peak asymmetry factor and erf{ } is an error function. For Eqn 2, $a_0$ is not the peak amplitude, but is proportional to the peak area $= 2a_0a_3$. Deconvolution of overlapping peaks may be performed by a simultaneous multiple non-linear curve-fitting program (PeakFit®), after manipulation of the experimental DSC data (heat flux as a function of temperature) using a spreadsheet program (e.g., Microsoft Excel®).

## Materials and Methods

(1*S*)-(+), (1*R*)-(−)- and (±)-camphorquinone (99%, Aldrich), (*R*)-(+)-, (*S*)-(−)- and (±)-propranolol hydrochloride (99%, Aldrich) and (*S*)-(+)-, (*R*)-(−)- and (±)-mandelic acid (99 + %, Aldrich) were used as received. Finely powdered physical mixtures of each pair of isomers were prepared in different compositions by very thorough grinding of accurately weighed (Cahn Model 2000 electromicrobalance) quantities of each isomer with an agate mortar and pestle. DSC scans

of 2–3 mg of each mixture were normally obtained at a heating rate of 2.0 K $min^{-1}$ with a Perkin-Elmer DSC-7 scanning calorimeter controlled by an IBM PS/2 Model 50 Z microcomputer (Elsabee and Prankerd, 1992). This computer was used for all data operations. $\Delta H_f^m$ values were obtained for the total area under each scan, using the Perkin-Elmer DSC-7 software. Modelling of the DSC endotherms was performed with PeakFit® (Version 2.0, Jandel Scientific, Corte Madera, CA), as previously described (Elsabee and Prankerd, 1992). Infrared (IR) spectra were obtained for 1–2 mg of the ground binary mixtures, carefully dispersed in pre-ground KBr (100 mg, Fisher, IR grade) and compressed in a 13 mm stainless-steel die at 5000 $lb/inch^2$ (Carver Laboratory Press, Fred S. Carver, Inc., Summit, NJ). Spectra were recorded with a Perkin-Elmer 1600 Fourier Transform (FT) Spectrophotometer, using 16 scans for each sample. The spectra were corrected by subtracting the spectrum of a blank pellet of KBr of equal mass and are presented in the absorption mode.

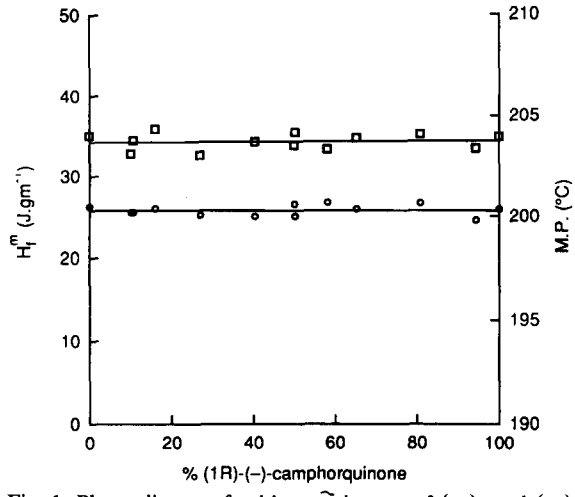


Fig. 1. Phase diagram for binary mixtures of (+)- and (−)-camphorquinone. $\Delta H_f^m$ values (□) and melting points (○) are plotted as a function of mol% composition.

## Results and Discussion

*Endotherm shapes for DSC scans of camphorquinone mixtures*

DSC scans of all mixtures of (1*S*)-(+)- and (1*R*)-(−)-camphorquinone displayed a single endotherm which exhibited a skewed distribution. As only a single peak was present, it was not necessary to fit these data with PeakFit®. The temperature at which melting was just complete (liquidus temperature) and the change in enthalpy for fusion ($\Delta H_f^m$) of each mixture were independent of composition (Fig. 1). This behavior is characteristic of a species which forms racemic solid solutions. The observed asymmetric endotherms suggested that the mixtures were nearly, but not completely, ideal. There was no marked dependence of asymmetry on composition, as discussed below for propranolol hydrochloride. Such composition-independent behavior has previously been observed for the melting

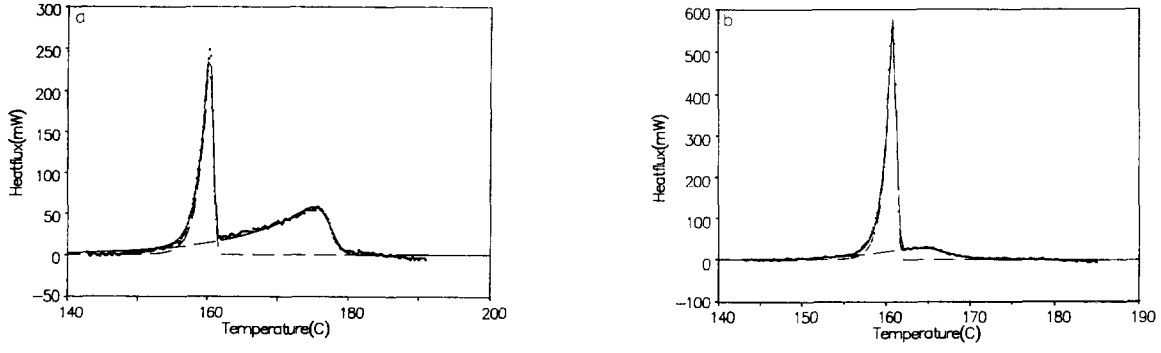


Fig. 2. PeakFit plots of DSC data for physical mixtures of (*R*)-(+)- and (*S*)-(−)-propranolol hydrochloride; (a) 28.74 mol% (*S*)-(−)-; (b) 44.45 mol% (*S*)-(−)-. (·····) Experimental points; (— — —) EMG curves; (———) summation curve (EMG curves plus plus linear background).

curves of other (+)- and (−)-camphor derivative mixtures (Ross and Somerville, 1926; Eliel, 1962).

*DSC scans of binary mixtures of (R)-(+)- and (S)-(−)-propranolol hydrochloride*

DSC scans of intimate physical mixtures of (*R*)-(+)- and (*S*)-(−)-propranolol hydrochloride displayed two endotherms which overlapped when the mole percent of one optical isomer was from 15 to 85%. Unlike the isomers of ephedrine hydrochloride (Elsabee and Prankerd, 1992), the endotherms are more separated on the temperature scale and are not superimposed for compositions outside the range 45–55%. Examples are given in Fig. 2. Both endotherms of each scan were fitted by PeakFit® to an EMG distribution better than to a Gaussian distribution. Peak centers, relative peak areas and the *F* ratio for each fit are given in Table 1. $\Delta H_f^m$ values were calculated for each peak from the ratio of peak areas to the total area and the total enthalpy of fusion, previously obtained from the Perkin-Elmer DSC-7 software. These are reported in Table 2. The *F* ratios listed in Table 1 represent highly significant fits to the experimental data ($p \ll 0.001$ in the worst case) (Rohlf and Sokal, 1969). The peak center ($a_1$) values in Table 1 are nearly constant for the lower melting of the two endotherms (peak 1), which corresponds to melting of the racemic mixture (eutectic).

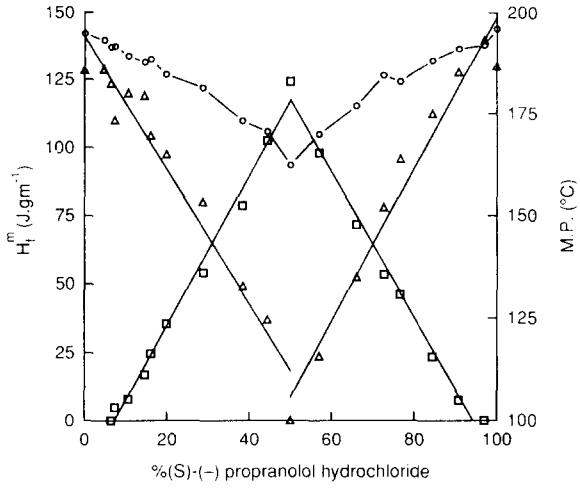


Fig. 3. $\Delta H_f^m$ values for the racemic mixture (□) and enantiomers (△) and the corresponding liquidus temperatures (○) as a function of mol% (*S*)-(−)-propranolol hydrochloride in physical mixtures of the two enantiomers. Correlation coefficients for the lines ranged from 0.98 to 0.995.

*DSC scans of binary mixtures of (S)-(+)- and (R)-(−)-mandelic acid*

DSC scans of the enantiomers of mandelic acid gave single, slightly asymmetric endotherms,

TABLE 1

*Peak centers ($a_1$) and relative endotherm areas for DSC scans of physical mixtures of (R)-(+)- and (S)-(−)-propranolol hydrochloride using the EMG model*

| % (*S*)-(−)- | *F* ratio | $a_1$ (peak 1) (°C) | Relative area (peak 1) | $a_1$ (peak 2) (°C) | Relative area (peak 2) |
|---|---|---|---|---|---|
| 14.54 | 3162 | 159.0 | 0.1211 | 184.6 | 0.8789 |
| 16.04 | 2784 | 161.6 | 0.1910 | 184.7 | 0.8090 |
| 19.88 | 9908 | 160.2 | 0.2658 | 181.1 | 0.7342 |
| 26.12 | 3759 | 160.7 | 0.3758 | 176.1 | 0.6242 |
| 28.74 | 8681 | 160.3 | 0.4036 | 175.0 | 0.5964 |
| 38.38 | 13355 | 160.6 | 0.6157 | 167.1 | 0.3842 |
| 44.45 | 14978 | 160.8 | 0.7345 | 163.9 | 0.2655 |
| 50.00 [a] | – | 160.9 | 1.000 | – | – |
| 56.93 | 10978 | 160.5 | 0.8056 | 164.9 | 0.1943 |
| 66.05 | 10816 | 160.6 | 0.5766 | 170.5 | 0.4234 |
| 72.69 | 5009 | 162.9 | 0.4068 | 176.2 | 0.5932 |
| 76.67 | 4916 | 160.5 | 0.3249 | 179.2 | 0.6751 |
| 84.41 | 7441 | 159.9 | 0.1653 | 184.4 | 0.8347 |

[a] Pure racemic (±)-propranolol hydrochloride.

as did the racemate. Scans of intimate, thoroughly ground physical mixtures of (*S*)-(+)- and (*R*)-(−)-mandelic acid displayed a more complex situation than that previously described for propranolol hydrochloride (this work) or ephedrine hydrochloride (Elsabee and Prankerd, 1992). In the range 100–98% of one enantiomer, a very asymmetric single endotherm was observed. Two overlapping endotherms were observed in the ranges 97.7–74 and 68–50%. A single endotherm with a very broad base was observed in the range 74–68%. The overlapping endotherms and the apparent single endotherm were deconvoluted by PeakFit® into two separate events, with the fractional areas and *F* ratios given in Table 3. The relative (fractional) areas and the total area were used to calculate $\Delta H_f^m$ values for each event (Table 4). The values for the liquidus temperature are also reported in Table 4. These data are plotted as a phase diagram in Fig. 4. As noted above for the propranolol hydrochloride data, PeakFit® gave highly significant *F* ratios for the fitted peaks ($p \ll 0.001$ in the worst case).

TABLE 2

*Changes in enthalpies for fusion ($\Delta H_f^m$, J g$^{-1}$) based on the relative areas in Table 1, and also the liquidus temperatures from DSC scans of physical mixtures of (R)-(+)- and (S)-(−)-propranolol hydrochloride*

| % (−)- | $\Delta H_f^m$ (peak 1) | $\Delta H_f^m$ (peak 2) | Liquidus temperature |
|---|---|---|---|
| 0.00 [b] | – | 128.45 | 194.6 |
| 4.74 [b] | – | 128.80 | 193.0 |
| 6.46 [b] | – | 123.50 | 191.3 |
| 7.37 | 4.90 | 110.10 | 191.4 |
| 10.68 | 7.90 | 120.00 | 189.0 |
| 14.53 | 16.80 | 119.00 | 187.5 |
| 16.03 | 24.62 | 104.38 | 188.2 |
| 19.88 | 35.40 | 97.38 | 184.5 |
| 28.74 | 54.07 | 79.92 | 181.2 |
| 38.38 | 78.62 | 49.07 | 173.2 |
| 44.45 | 102.43 | 37.03 | 170.5 |
| 50.00 [a] | 124.05 | – | 162.3 |
| 56.93 | 97.96 | 23.63 | 169.9 |
| 66.05 | 71.49 | 52.50 | 176.8 |
| 72.69 | 53.45 | 77.94 | 184.3 |
| 76.67 | 46.08 | 95.76 | 182.8 |
| 84.41 | 23.44 | 112.52 | 188.0 |
| 90.79 [b] | 7.50 | 127.77 | 190.9 |
| 96.97 [b] | 0.00 | 139.63 | 191.8 |
| 100.00 [b] | – | 129.90 | 195.9 |

[a] Pure racemic (±)-propranolol hydrochloride.
[b] Endotherms had baseline separation and did not require deconvolution.

The phase diagram based on $\Delta H_f^m$ values (Fig. 4) is readily interpreted in terms of racemic compound formation with a maximum at 50% and eutectic points corresponding to mixing of the racemic compound with each of the enantiomers at about 29 and 71% of (*S*)-(+)-mandelic acid. These points are calculated from simultaneous solution of the regression coefficients for the lines intersecting at the theoretical 1:1 composition and the eutectic points (Table 5). The calculated composition for the 1:1 racemic compound (49.8–50.1%) (Table 6) is extremely close to the theoretical value of 50.0%. There is very good agreement between the two estimates for each eutectic point (Table 6). The ready interpretaton of this phase diagram is in strong contrast to the vague nature of the diagram derived from liquidus temperatures. That plot could probably be interpreted as demonstrating racemic compound formation, but location of the eutectic points would be very arbitrary. The plot of liquidus temperatures is not as symmetrical as might be expected for such a system, while the plots of $\Delta H_f^m$ values are extremely so, based on the regression coefficients in Table 5.

It is noteworthy that the $\Delta H_f^m$ values for the racemic compound (176.1 J g$^{-1}$) and the enantiomers (168.5–169.1 J g$^{-1}$) are almost identical, while the melting points are rather different (117.8 °C compared to 129.4–129.6 °C, respectively). These data would suggest that the racemic compound is more water-soluble than the enantiomers.

In the composition range 90–74%, multiple overlapping events, including an exotherm, were observed if grinding was not thorough. At heating rates from 1.0 to 20.0 K min$^{-1}$, the endotherm preceding the exotherm became more pronounced at faster heating rates. These phenomena indicate a polymorphic phase transition. Polymorphism has previously been reported for racemic mandelic acid (Kuhnert-Brandstätter and Ulmer, 1974). The melting temperature for the racemic compound was about 120 °C, while the

eutectic melting temperature in the present study was 115–116 °C. This corresponds to the previously reported form I of the racemic compound (racemate I), which is more stable than form II (racemate II) (Kuhnert-Brandstätter and Ulmer, 1974). The IR spectra in this study are also in agreement with the assignment of form I.

Plotting $\Delta H_f^m$ values as a function of mol% composition resulted in linear traces which were easier to interpolate and extrapolate than standard plots of liquidus temperatures, which are often curved (Patel and Hurwitz, 1972; Prankerd and Ahmed, 1992) or indeterminate (present work, Fig. 4). The melting phase diagram for mandelic acid, especially the eutectic points, was not made clear until the 1970's (Kuhnert-Brandstätter and Ulmer, 1974). The eutectic points from the present approach are in very close agreement with those previously reported. Comparison of the plots for liquidus temperatures and $\Delta H_f^m$ values in Fig. 4 demonstrates the ease of interpretation by this approach.

*IR spectra of binary mixtures of (S)-(+)- and (R)-(−)-mandelic acid*

The enantiomers of mandelic acid gave IR spectra which differed from that of the racemic compound. IR absorbance spectra of intimate, thoroughly ground physical mixtures of (*S*)-(+)- and (*R*)-(−)-mandelic acid displayed several bands which changed intensity as a function of composition (Fig. 5). A spectrum of the authentic racemic compound was identical to that of a ground mixture of (*S*)-(+)- and (*R*)-(−)-mandelic

TABLE 3

*Peak centers ($a_1$) and relative endotherm areas for DSC scans of physical mixtures of (R)-(−)- and (S)-(+)-mandelic acid using the EMG model*

| % (*S*)-(+)- | *F* ratio | $a_1$ (peak 1) (°C) | Relative area (peak 1) | $a_1$ (peak 2) (°C) | Relative area (peak 2) |
|---|---|---|---|---|---|
| 5.00 | 4393 | 114.7 | 0.1405 | 129.2 | 0.8595 |
| 10.24 | 10062 | 115.1 | 0.2791 | 125.7 | 0.7209 |
| 12.60 | 13683 | 115.2 | 0.3069 | 125.0 | 0.6931 |
| 15.56 | 4420 | 115.6 | 0.5378 | 121.0 | 0.4622 |
| 16.96 | 3150 | 112.9 | 0.4289 | 119.1 | 0.5711 |
| 22.73 | 22184 | 112.7 | 0.6926 | 115.6 | 0.3073 |
| 29.36 | 8129 | 115.0 | 0.9374 | 115.3 | 0.0626 |
| 33.15 | 19959 | 113.2 | 0.7570 | 113.9 | 0.2430 |
| 35.30 | 7470 | 112.9 | 0.6317 | 114.5 | 0.3683 |
| 40.25 | 5455 | 112.4 | 0.3621 | 115.3 | 0.6379 |
| 44.87 | 14111 | 115.1 | 0.3000 | 118.5 | 0.7000 |
| 45.73 | 11691 | 113.0 | 0.2541 | 116.4 | 0.7459 |
| 49.95 | 2117 | 114.7 | 0.0290 | 119.6 | 0.9710 |
| 51.76 | 3311 | 113.1 | 0.0920 | 118.0 | 0.9080 |
| 53.80 | 21898 | 112.0 | 0.2000 | 116.5 | 0.8000 |
| 55.88 | 16974 | 112.5 | 0.2823 | 116.1 | 0.7177 |
| 56.44 | 12547 | 115.4 | 0.3196 | 118.9 | 0.6804 |
| 59.29 | 3089 | 113.3 | 0.4316 | 116.0 | 0.5684 |
| 60.11 | 22125 | 115.0 | 0.3659 | 118.2 | 0.6341 |
| 62.31 | 8271 | 116.2 | 0.6811 | 117.7 | 0.3189 |
| 68.70 | 31462 | 112.9 | 0.6390 | 112.8 | 0.3610 |
| 69.07 | 5815 | 113.3 | 0.7964 | 114.3 | 0.2035 |
| 71.42 | 2802 | 115.8 | 0.9516 | 117.5 | 0.0484 |
| 74.87 | 13415 | 115.6 | 0.8396 | 117.4 | 0.1604 |
| 76.80 | 2071 | 116.4 | 0.7936 | 118.6 | 0.2064 |
| 80.53 | 8641 | 112.6 | 0.6099 | 116.4 | 0.3901 |
| 86.86 | 4926 | 115.1 | 0.3385 | 123.9 | 0.6615 |

[a] Pure racemic (±)-mandelic acid.

TABLE 4

*Changes in enthalpies for fusion ($\Delta H_f^m$, J $g^{-1}$) based on the relative areas in Table 3, and also the liquidus temperatures from DSC scans of physical mixtures of (R)-(−)- and (S)-(+)-mandelic acid*

| % (S)-(+)- | $\Delta H_f^m$ (peak 1) | $\Delta H_f^m$ (peak 2) | Liquidus temperature |
|---|---|---|---|
| 0.00 [b] | 0.00 | 169.09 | 131.5 |
| 2.32 [b] | 5.36 | 151.52 | 131.8 |
| 5.00 | 23.00 | 140.78 | 130.5 |
| 10.24 | 48.34 | 124.88 | 128.7 |
| 12.60 | 51.93 | 117.25 | 127.9 |
| 15.56 | 93.00 | 80.84 | 126.6 |
| 22.73 | 119.13 | 52.80 | 120.7 |
| 29.36 | 158.49 | 11.30 | 115.9 |
| 33.15 | 119.21 | 38.26 | 114.8 |
| 35.30 | 104.94 | 61.18 | 116.0 |
| 40.25 | 58.48 | 103.03 | 116.3 |
| 44.87 | 52.39 | 122.23 | 119.1 |
| 45.73 | 41.90 | 125.41 | 116.9 |
| 49.95 | 5.03 | 168.73 | 120.1 |
| 50.00 [a] | 0.00 | 176.10 | 120.6 |
| 51.76 | 15.33 | 151.25 | 118.4 |
| 53.80 | 32.52 | 130.06 | 117.2 |
| 55.88 | 46.32 | 117.78 | 116.7 |
| 56.44 | 53.20 | 113.30 | 119.5 |
| 59.29 | 60.53 | 112.75 | 117.0 |
| 60.11 | 61.54 | 106.60 | 118.8 |
| 62.79 | 108.65 | 50.80 | 118.8 |
| 67.96 | 120.25 | 45.00 | 119.4 |
| 69.07 | 131.50 | 33.61 | 118.4 |
| 71.42 | 156.20 | 7.90 | 120.9 |
| 74.87 | 140.00 | 26.74 | 120.7 |
| 80.53 | 99.46 | 63.60 | 120.9 |
| 83.45 | 85.77 | 82.50 | 124.0 |
| 85.30 | 69.40 | 100.60 | 125.6 |
| 86.86 | 54.15 | 105.81 | 127.2 |
| 86.97 | 54.15 | 105.80 | 126.8 |
| 90.34 | 45.00 | 121.28 | 128.5 |
| 93.13 | 16.44 | 143.61 | 129.5 |
| 96.95 | 10.90 | 149.60 | 129.4 |
| 97.69 [b] | 0.00 | 166.13 | 132.2 |
| 99.09 [b] | 0.00 | 166.37 | 132.8 |
| 100.00 [b] | 0.00 | 168.50 | 131.9 |

[a] Pure racemic (±)-mandelic acid.

[b] Endotherms had baseline separation and did not require deconvolution.

acid in equal proportions. Of special interest is the associated benzylic O-H stretching band at 3447 $cm^{-1}$ in the enantiomers, which was replaced by one at 3405 $cm^{-1}$ in the racemic compound. This band shift clearly indicated a change

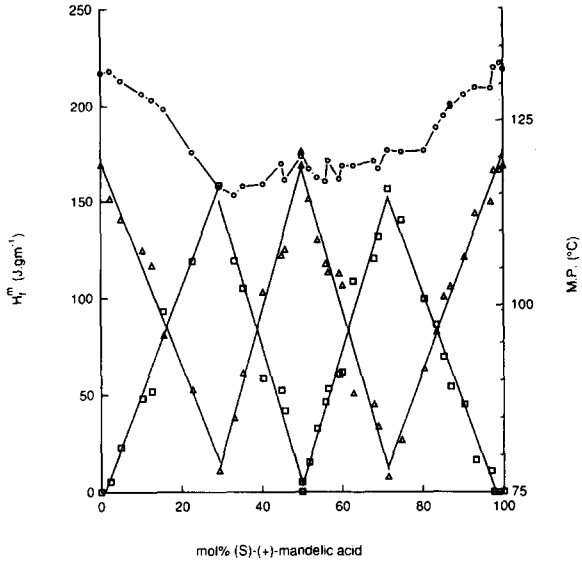


Fig. 4. Solid-liquid phase diagram for mandelic acid. $\Delta H_f^m$ values for endotherm 1 (low melting) (□) and endotherm 2 (high melting) (△) and the corresponding liquidus temperatures (○) are plotted as a function of mol% (S)-(+)-mandelic acid in physical mixtures of the two enantiomers. Correlation coefficients for the lines ranged from 0.973 to 0.994.

TABLE 5

*Regression coefficients for the mandelic acid phase diagram*

| Composition range (%) | Intercept | Slope | Correlation coefficient ($r^2$) |
|---|---|---|---|
| Endotherm 1 | | | |
| 0– 29 | −5.2952 | 5.5374 | 0.992 |
| 29– 50 | 356.86 | −7.0432 | 0.988 |
| 50– 71 | −342.69 | 6.9179 | 0.988 |
| 71–100 | 558.36 | −5.6927 | 0.991 |
| Endotherm 2 | | | |
| 0– 29 | 170.21 | −5.2469 | 0.990 |
| 29– 50 | −209.99 | 7.566 | 0.993 |
| 50– 71 | 524.9 | −7.1809 | 0.977 |
| 71–100 | −393.37 | 5.6884 | 0.994 |

TABLE 6

*Calculated eutectic points and racemate composition from the mandelic acid phase diagram*

| | 1st eutectic (%) | Racemate (%) | 2nd eutectic (%) |
|---|---|---|---|
| Endotherm 1 | 28.79 | 50.11 | 71.45 |
| Endotherm 2 | 29.67 | 49.83 | 71.35 |

in hydrogen bonding in the crystal structure. These differences are suggestive of changes occurring in the intermolecular arrangement of the crystal unit cell. Bands characteristic of the molecular skeletal structure, e.g., benzylic C-O stretch (1075 $cm^{-1}$) or methylene C-H deformation (1454 $cm^{-1}$), were essentially unchanged. The gradual formation of new bands as a function of composition (rather than displacement of existing bands) indicates that the ground binary mixtures contained both the racemic compound and the enantiomer in excess. Formation of the racemic compound must have occurred during grinding of the two enantiomers, as the ground mixtures were gently incorporated into the finely powdered KBr, and not ground with it. Changes in band intensity, relative to the intensity of the carbonyl stretching band (C=O stretch, 1716 $cm^{-1}$) are shown in Fig. 6 for several representative bands.

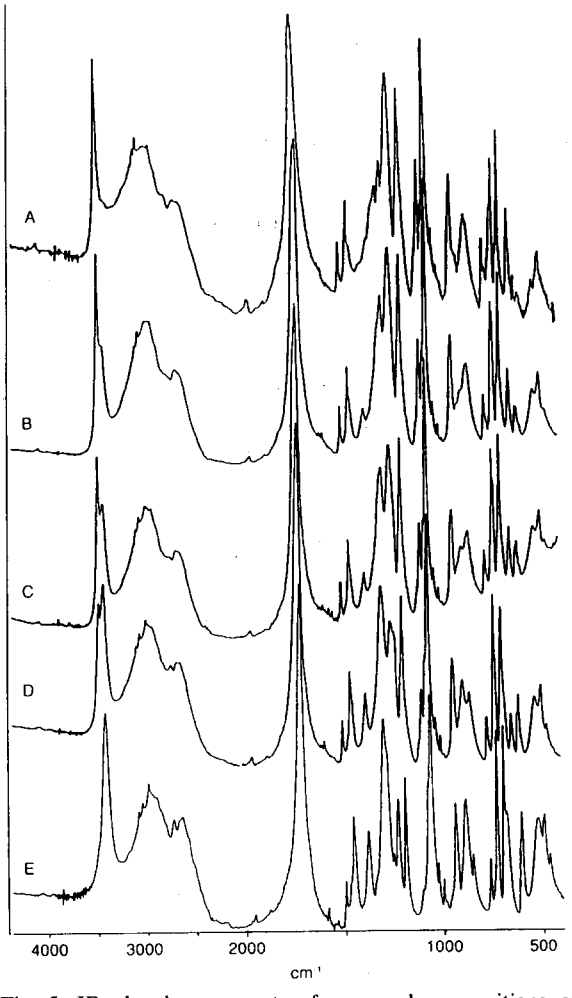


Fig. 5. IR absorbance spectra for several compositions of (*S*)-(+)- and (*R*)-(−)-mandelic acid. (A) 100%; (B) 85.94%; (C) 79.56%; (D) 69.79%; and (E) 50.28% (*S*)-(+)-mandelic acid.

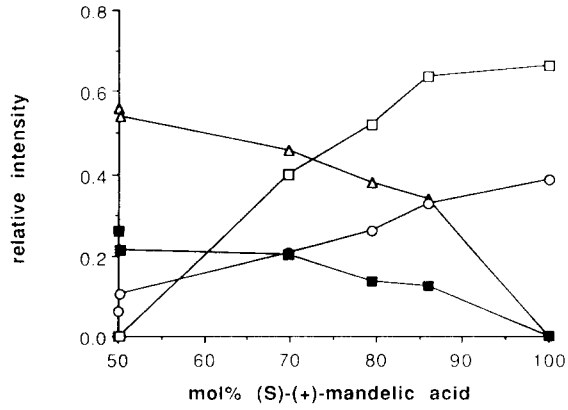


Fig. 6. Changes in IR absorbance band intensity as a function of mol% (*S*)-(+)-mandelic acid for several band positions. (□) 3447 $cm^{-1}$; (△) 3405 $cm^{-1}$; (■) 1377 $cm^{-1}$; (○) 1097 $cm^{-1}$.

Although changes in crystalline polymorphic form caused by grinding have been reported several times (Cleverley and Williams, 1959a, b; Kaneniwa and Otsuka, 1985), the formation of racemic compounds from their constituent enantiomers, without passing through an intermediate melted or solution phase, does not appear to have been reported. It is possible that the transition from pure enantiomers to form I occurs through the less stable form II, which has been reported to have a similar IR spectrum to that of the enantiomers. This suggestion is supported by the observation of multiple thermal events, including exotherms, when the mixtures were not thoroughly ground. Confirmation of the transition from enantiomer mixture to the racemic compound form I, through form II, might be possible by X-ray powder diffraction methods. All three species might be expected to have some differences in their powder diffraction patterns.

*Minor component detection in chiral mixtures*

For physical compositions of propranolol hydrochloride near to that of the pure enantiomers (> 92.5%), only a single peak was observed by DSC. This is indicated in the phase diagram (Fig. 3) by the $x$-intersections of the regression lines for the racemic mixture (open squares). It is possible that solid solutions may be formed for these compositions (92.5–100%). This observation is in contrast to previous reports on other chiral drugs (Bettinetti et al., 1990; Elsabee and Prankerd, 1992), in which the presence of 1.5% (or possibly less) of one isomer could be detected in the other. Hence, propranolol hydrochloride is an example of a chiral drug for which quantification of small amounts of one enantiomer in an excess of the other (e.g., for quality control purposes) would not be possible by DSC detection of eutectic melting. However, it was noted that mixtures which gave single endotherms only (92.5–100%) were increasingly asymmetric. The peak asymmetry factor ($a_3$) was estimated (using PeakFit®) for all scans displaying a single endotherm only, as well as for several in which the second endotherm was also present. Data were used where either (*S*)-(−)- or (*R*)-(+)-propranolol hydrochloride was the minor component. These data are shown in Table 7 as a function of composition and are plotted in Fig. 7. They show that a single linear relationship ($r^2 = 0.981$) exists between the asymmetry factor and the composition in the range 85–100 mol%, irrespective of which enantiomer is in excess. The relationship breaks down for lower percentages. However, in this region (15–85 mol%), the composition could be estimated by reference to the phase diagram. Propranolol hydrochloride (racemic) has been reported to have two polymorphs (Kuhnert-Brandstätter and Völlenklee, 1985). However, as these two modifications were reported to be very similar in thermal properties, it is unlikely that any major discrepancies would arise from this cause.

The use of DSC for purity analysis, by employing a modified form of the van 't Hoff isochore to analyze the melting endotherm, was first suggested in 1966 (Wendlandt, 1986). This approach is usually applicable to materials with a mol% purity in the range 97–100%. It is noteworthy that the analysis described in the present work, at least in this case, could be used to estimate chiral purity in samples containing up to 15 mol% of the minor component. Provided that the peak

TABLE 7

*Peak asymmetry factor as a function of mol% composition for binary mixtures of (S)-(−)- and (R)-(+)-propranolol hydrochloride*

| Enantiomer in excess | mol% of major component | Asymmetry factor ($a_3$) |
|---|---|---|
| *S* | 100.00 | 0.7723 |
| *R* | 100.00 | 0.6254 |
| *S* | 96.97 | 1.4606 |
| *R* | 95.26 | 2.7963 |
| *R* | 93.53 | 2.9357 |
| *R* | 93.30 | 3.0497 |
| *R* | 92.63 | 3.1404 |
| *S* | 90.79 | 4.7380 |
| *R* | 89.31 | 5.9400 |
| *R* | 87.94 | 5.3927 |
| *R* | 85.46 | 7.9042 |
| *S* | 84.41 | 8.0376 |
| *S* | 76.67 | 9.2976 |
| *S* | 72.69 | 9.3064 |
| *S* | 66.05 | 6.6734 |

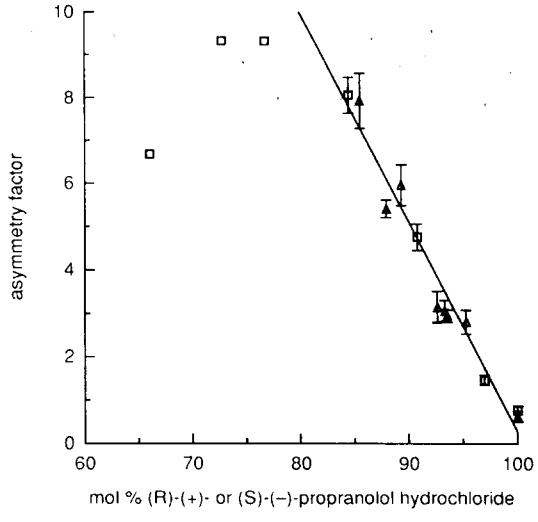


Fig. 7. Relationship between mol% composition of (*R*)-(+)- and (*S*)-(−)-propranolol hydrochloride mixtures, and peak asymmetry factor for the DSC melting endotherm. (□) (*S*)-(−)- in excess; (△) (*R*)-(+)- in excess.

asymmetry of a mixture of known impurity content is estimated at the same time (to establish the slope of the relationship), chiral purity estimation in practice could be achieved over a much wider range than that possible by the standard DSC method. The time required for this purity estimate would still be less than that required to set up a chiral HPLC separation, let alone establishing the validity of such a separation. It is expected that these two approaches should be largely complementary in quantitative analysis of mixtures of chiral substances.

The DSC approach described in this paper, combined with independent, non-chiral HPLC analysis (to exclude non-chiral contaminants), could allow rapid quantification of the minor component in such mixtures, for quality control purposes. Detection of about 2% of either of the mandelic acid enantiomers (as the racemic compound) in the presence of about 98% of the other was possible by DSC observations of eutectic melting. However, detection of smaller amounts than 2% would depend on quantitative analysis of peak asymmetry, as suggested above for propranolol hydrochloride.

## Acknowledgements

This study was funded by a University of Florida DSR Research Development Award. Additional financial support was given by SmithKline Beecham.

## References

Bettinetti, G., Giordano, F., Fronza, G., Italia, A., Pellegata, R., Villa, M. and Ventura, P.., Sobrerol enantiomers and racemates: Solid state spectroscopy, thermal behavior and phase diagrams. *J. Pharm. Sci.*, 79 (1990) 470–475.

Cleverley, B. and Williams, P.P., Polymorphism and changes of infrared spectra of barbiturates during sample preparation. *Chem. Ind.*, (1959a) 49–50.

Cleverley, B. and Williams, P.P., Polymorphism in substituted barbituric acids. *Tetrahedron*, 7 (1959b) 277–288.

Eliel, E.L., *Stereochemistry of Carbon Compounds*, McGraw-Hill, New York, 1962, pp. 43–47.

Elsabee, M. and Prankerd, R.J., Solid-state properties of drugs. II. Peak shape analysis and deconvolution of overlapping endotherms in differential scanning calorimetry of chiral mixtures. *Int. J. Pharm.*, 86 (1992) 211–219.

Hutt, A.J., Drug chirality: impact on pharmaceutical regulation. *Chirality*, 3 (1991) 161–164.

Kaneniwa, N. and Otsuka, M., Effect of grinding on the transformations of polymorphs of chloramphenicol palmitate, *Chem. Pharm. Bull.*, 33 (1985) 1660–1668.

Kuhnert-Brandstätter, M. and Ulmer, R., Beitrag zur thermischen Analyse optischer Antipoden: Mandelsäure. *Mikrochim. Acta (Wien)*, (1974) 927–935.

Kuhnert-Brandstätter, M. and Völlenklee, R., Thermoanalytische und IR-spectroskopische Untersuchungen an polymorphen Arzneistoffen. *Fresenius' Z. Anal. Chem.*, 322 (1985) 164–169.

Patel, R.M. and Hurwitz, A., Eutectic temperature determination of preformulation systems and evaluation by controlled freeze drying. *J. Pharm. Sci.*, 61 (1972) 1806–1810.

Prankerd, R.J. and Ahmed, S.M., Physicochemical interactions involving praziquantel, oxamniquine and tablet excipients. *J. Pharm. Pharmacol.*, 44 (1992) 259–261.

Rohlf, F.J. and Sokal, R.R., *Statistical Tables*, Freeman, San Francisco, 1969, pp. 168–197.

Ross, A.J. and Somerville, I.C., Melting point curves of optical isomerides in the camphor series. *J. Chem. Soc.*, 128 (1926) 2770–2784.

Wendlandt, W.W., *Thermal Analysis,* Wiley, New York, 1986, Ch. 10.